A COMPREHENSIVE CAUSE ANALYSIS OF A COUPLING FAILURE INDUCED BY TORSIONAL OSCILLATIONS IN A VARIABLE SPEED MOTOR

by

Harley Tripp

Senior Staff Engineer

Don Kim

Associate Research Engineer

Shell Development Company

Houston, Texas

and

Robert Whitney

Project Engineer

Lucas Power Transmission Company

Utica, New York

Harley Tripp, a Senior Staff Engineer in the Mechanical Engineering Department of Shell Development Company, has worked on a wide range of mechanical engineering problems related to the petroleum industry. He is the author or coauthor of more than a dozen technical society papers dealing with rotordynamics, bearing lubrication, and artificial lift, and has developed several computer programs which Shell licenses to other companies. Mr. Tripp has spent the past several years working on reliability programs for improving the availability of Shell's refineries.

He joined Shell (1966) after receiving his B.S. and M.S. degrees in Mechanical Engineering from the University of Mississippi. Mr. Tripp is a licensed Professional Engineer in Texas and is a member of ASME, SPE, and Sigma Xi.

Don Kim is an Associate Research Engineer in the Department of Pressure Equipment Integrity, Shell Development Company. His specialties are in the areas of fitness for service, fracture mechanics, and welding engineering. Prior to joining Shell (1990), he was a Lecturer at the Ohio State University.

Mr. Kim graduated from Seoul National University (B.S. and M.S.) and taught in the Department of Marine Mechanical Engineering, Yeungnam University for five years. He earned his Ph.D. degree at the Ohio State University, Department of Welding Engineering in 1989.

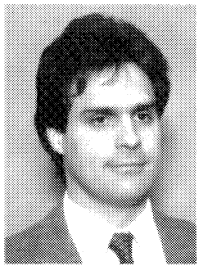

Robert (Bob) Whitney is a Project Engineer in charge of coupling design at Lucas Aerospace Power Transmission Corporation, Utica, New York.

Mr. Whitney earned a B.S. in Mechanical Engineering (1983) at the State University of New York at Buffalo. He is a registered Professional Engineer in New York and is an associate member of ASME.

ABSTRACT

The analysis of two compressor train coupling failures that were caused by a subsynchronous torsional resonance is discussed. These torsional failures manifested themselves as fatigue cracks that propagated across the coupling spacers at a classic 45 degree orientation.

Analysis of the failures included a long term program of measuring actual online coupling stresses, identifying the source of the infrequent subsynchronous torsional oscillations, a finite element analysis of the coupling, and a fracture mechanics analysis which, along with measured stresses, explained the failures.

BACKGROUND

Both couplings that failed were the motor-to-gearbox couplings on a hydrogen makeup compressor in one of Shell's refineries. As shown in Figure 1, the compressor train consists of a variable speed motor, a gearbox that increases the motor speed by a factor of 4.62 ratio, and two compressor cases in series. The compressor train was initially installed in 1967 with a 1780 rpm electric motor rated at 6,900 hp. In 1985 the train system was reconfigured, using a new variable speed motor with an operating speed range of 1270 to 1825 rpm. At the same time, the original gears with a 5.225 ratio were replaced with new gears with a 4.62 ratio.

During the 1985 installation, new flexible diaphragm couplings [1] were installed in the train. At the time these couplings were

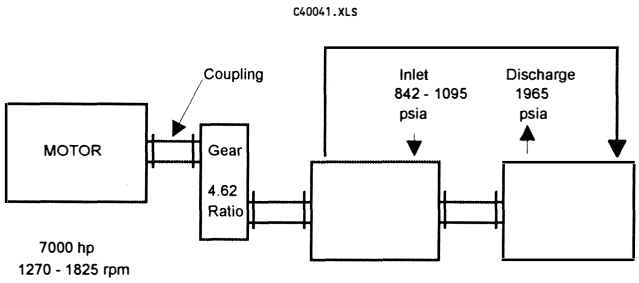

Figure 1. Hydrogen Makeup Compressor Train Showing the Location of the Coupling Failures.

installed, flexible diaphragm couplings had been successfully used on compressor trains within Shell for almost a decade.

The coupling had been in service for almost five years when the first coupling failure occurred in February 1990. The failure was discovered as a result of high radial vibration caused by unbalance as the crack opened. A second failure occurred a year later. In both cases the failure mode was a torsional fatigue crack that initiated at the welded junction of the coupling tube and diaphragm and propagated into both the tube and coupling.

INTRODUCTION

At the time the failure occurred, the importance of torsional slip frequencies in variable speed motors was not widely known [2, 3]. Consequently, in the fall of 1991, a root cause analysis study was started on the two coupling failures. This analysis included systematically investigating both the failure mechanism and the external forces that acted on the coupling to cause the coupling stresses.

Cause Analysis Method

The *Technically Oriented Cause Analysis* method used in this investigation was a very focused cause analysis procedure that incorporated engineering analysis and measurements into the *Conventional Cause Analysis* structure documented by Kepner and Tregoe [4]. The method consisted of three tasks:

- *Problem Identification* involved selecting and defining the problem to be analyzed.
- *Cause Identification* involved carefully defining the failure mode so that the cause could be identified and verified — and then proceeding to the next level where the procedure of defining the effect and identifying the cause was repeated.
- *Final Verification* assured:
  - that the failure mode and mechanism, along with the component strength and forces acting on the component explained the failure.
  - that the causes actually existed.

In this investigation, *Final Verification* used the results of the failure mechanism analysis, which is the coupling fatigue strength shown later in Figure 5, with the high amplitude measurements recorded during two months to show that the number and amplitude of torsional cycles present during a year were sufficient to cause the cracks in the couplings.

The cause identification investigation followed two interwoven paths. The first path, investigated the coupling fatigue strength, and included the effects of manufacturing methods, size, design, and defects such as cracks. The second path pursued the external forces that acted on the coupling. Key questions asked during this task included:

- What were the number and amplitude of stress cycles in the coupling that caused the failure? What was the fatigue strength of the coupling that corresponded to the number of high amplitude torsional stress cycles the coupling experienced?
- What were the sources of the forces acting on the coupling that caused the stresses in the coupling?

COUPLING DESIGN ANALYSIS

Diaphragm type couplings have been successfully used since the 1970s and operate on machinery trains that range from several thousand hp to trains with over 60,000 hp. Prior to these failures, the few failures that had occurred had resulted from corrosion or from a single torsional overload. Results of the design analysis show that the coupling design was conservative and failures should not have been expected, since normally acceptable design practices and parameters were used.

Design Parameters

Coupling diaphragms and tubes were made of A4340 steels, which have a tensile strength of 130,000-150,000 psi. A tensile strength (S_u) of 130,000 psi and a yield strength (S_y) of 117,000 psi were used in the original design calculations, along with the other values given in Table 1. Speed and torque ratings were based on the projected use of the coupling, rather than on actual coupling capacity, which was 527,000 in-lbs and 19,500 rpm.

Rather than use the original design values, this analysis used a torque of 245,000 in-lbf, which corresponds to the current maximum motor rating of 7,000 hp at 1,800 rpm. Stresses in the coupling tube were calculated using:

$$S_m = \frac{\text{Torque}}{Z_o} \tag{1}$$

where:

$$Z_o = \frac{\Pi(D_{od}^4 - D_{id}^4}{16D_{od}} \tag{2}$$

Calculations using the current maximum motor torque and the polar section modulus (Z_o) from Table 1, found a stress (S_m) in the coupling tube of 6,860 psi.

Shearing stresses in the diaphragm were calculated using:

$$\sigma = \frac{P}{A} \tag{3}$$

where:

σ = stress

P = load

A = area.

Equation (3) with the maximum continuous same torque and the diaphragm dimensions resulted in a shearing stress in the diaphragm of 7,800 psi. As expected, the stresses in the tube and in the diaphragm were approximately equal, which explains why the crack propagated into both the tube and diaphragm.

Torsional Fatigue

Peak-to-peak torsional stresses equal to the maximum continuous design torque (245,000 in-lb) were used to evaluate the possibility of torsional fatigue in the coupling. Although this is very high for sustained cyclic loads, it provided a check on the coupling design.

Table 1. Coupling Specifications.

DESIGN HP
normal - 4032 hp
max cont - 6000
DESIGN SPEED
normal - 1528 rpm
max cont - 1800
min cont - 1444
trip limit - 19500
SIZE
Tube I.D. - 5.0 inch
Tube O.D. - 6.42
$Z_\bullet$ = 35.7 in^3

A material fatigue limit (S_n) of 37,700 psi was calculated using the ultimate tensile strength (S_u), and the relationship:

$$S_n = (0.5)(0.58)(S_u) \quad (4)$$

Equation (4), is based on a fatigue limit for reversed bending that is 0.5 times the ultimate tensile strength [5]. And, for reversed torsional stresses, the endurance limit is approximately 58 percent of the bending endurance limit.

A fatigue diagram is shown in Figure 2 for combining alternating and mean torsional stresses[6]. With a peak torque of 122,500 in-lbf and a SCF of 1.0, the peak torsional stress of 3,430 psi shown by point (1) on Figure 2 is substantially below the torsional fatigue limit of 37,700 psi. A finite element analysis, discussed later, found the couplings had a stress concentration factor (SCF) of 3.6 at the tube-to-diaphragm connection. This increased the peak torsional stresses to 12,350 psi shown by point (2). But, even this higher number represents a conservative design.

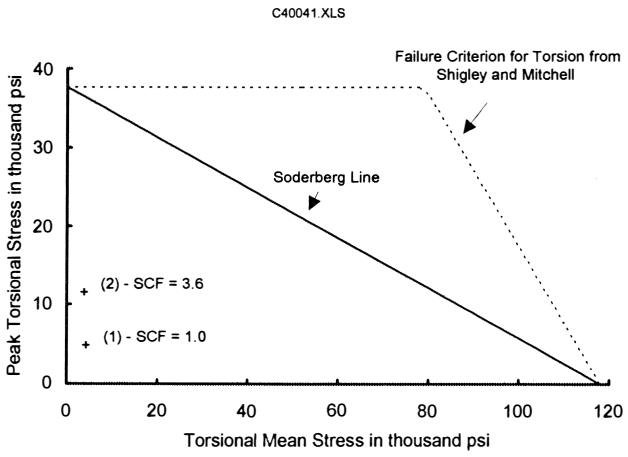

Figure 2. Fatigue Diagram Showing the Peak Coupling Stresses Based on the Maximum Motor Torque of 210,000 in-lbf.

FAILURE MECHANISM ANALYSIS

Failure Mode

Characteristics of the two coupling failures were similar. They did not result from the commonly encountered coupling failure modes of corrosion or from a single torsional overload incident. In both cases, the cracks propagated across the spool tube at an angle of 45 degrees, which is normally associated with torsional fatigue.

Metallurgical Analysis

The cracks started at the axial electron beam welds that connected the coupling tube and diaphragm, shown in Figure 3, and spread into both the tube and coupling. Metallographic examination identified the crack origins as welding inclusions at the roots of the welds that were 0.03 and 0.06 in deep. Fatigue striations in the vicinity of the origin are shown in Figure 4.

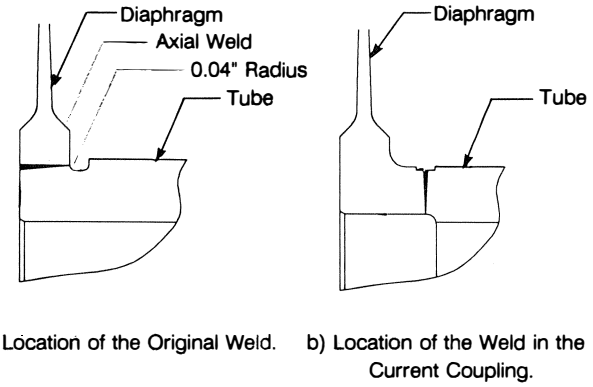

Figure 3. Location of the Coupling Diaphragm-to-Tube Weld Where the Failure Started.

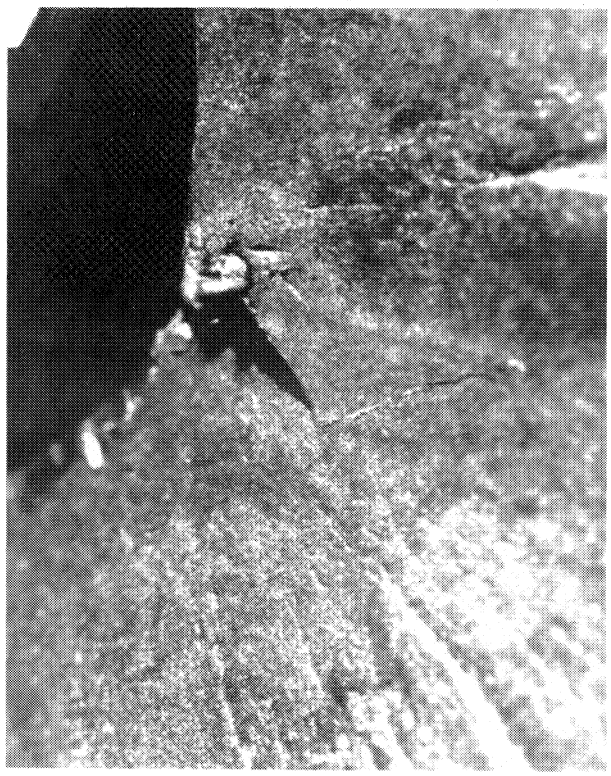

Figure 4. Fracture Surface of the First Coupling Failure Showing Fatigue Striations.

Spacing of the crack striations indicated that each coupling experienced more than a thousand, but less than a million high amplitude torsional stress cycles before the failures occurred. This

means that the failures did not result from the low number of torque cycles encountered during the compressor startups. Nor did the failures result from synchronous forces, which resulted in 2.3 million cycles per day. Fractography was unsuccessfully used in an attempt to obtain a better estimate of the number of cycles that caused the failures.

Finite Element Analysis

As previously discussed, the failures originated at the connection between the coupling spool tube and the diaphragm. The radius (r) of the shoulder fillet at the tube-to-diaphragm junction measured on the first coupling failure was 0.040 in, which was within the manufacturer's requirement of 0.040 to 0.050 in. The 0.006 ratio, of the fillet radius (r) to the 6.4 in tube diameter (d) (see the insert in Figure 3), is outside the range of SCFs that appear in standard references [7, 8]. Consequently, a finite element analysis was used to calculate the SCF at the this shoulder fillet where the crack originated. A finite element analysis calculated a SCF of 3.6 to 3.8 at this point.

Fracture Mechanics Analysis

Fracture mechanics principles were used to estimate the number of cycles at various stress ranges that were required for the weld inclusion to propagate. Fatigue crack propagation rates under cyclic stresses can be empirically represented[9] by the equation:

$$da/dN = A(\Delta K)^n \quad (5)$$

where:

da/dN is the crack growth rate

a = crack length, in

N = number of cycles

ΔK = stress-intensity-factor range, ksi $\sqrt{in}$

A and n are constants for a given material

for A4340 steel

A = 9.48 E-10

n = 2.67

and for steel with a ratio of minimum stress to maximum stress of 0.5, the threshold intensity factor range is [10],

$$\Delta K_{th} = 3.8 \text{ Ksi } \sqrt{in}$$

A computer program based on Equation (5), with a semielliptical crack in a cylinder was used to evaluate fatigue lives for various initial crack sizes and SCFs. The effect of startups on the fatigue life was also studied, with the conclusion that the precycle due to startups showed little effect on the coupling failures. Fatigue life is shown in Figure 5 for various stress ranges with three crack depths measured and a SFC of 3.6. These curves show the dynamic maximum stress range that will not result in failure due to crack propagation, as a function of the number of cycles. For example, the initial crack 0.06 in deep, would have required 50,000 cycles with a peak-to-peak dynamic stress range over 12,000 psi to cause the fatigue failure.

The threshold stress intensity factor range was used to calculate the minimum stress range for a crack to grow. A peak-to-peak stress range of 3,000 psi is needed for the 0.06 in weld inclusion to grow. This means that when the peak-to-peak stress level was less than 3,000 psi, the weld inclusion in the coupling did not increase in size.

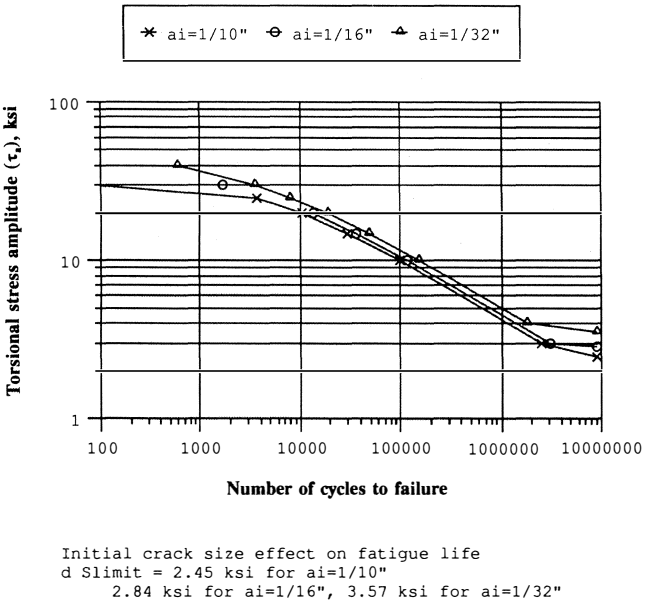

Figure 5. Fracture Analysis of the Coupling Material with Three Crack Depths and a Stress Concentration Factor of 3.6.

FORCES ACTING ON THE COUPLING

Misalignment

Axial and offset coupling misalignment contribute to the fluctuating stresses in diaphragm couplings. To assure that misalignment does not cause excessive fluctuating stresses, the coupling manufacturer specifies a maximum 0.20 degrees of nonparallel angular misalignment and 0.065 in of axial misalignment for each diaphragm. Measurements taken during the last turnaround indicate that the coupling alignment was well within this tolerance.

Calculated Torsional Natural Frequencies

Before the new motor was installed in 1985, several studies by outside consultants had been conducted to calculate the torsional critical speeds of the motor/coupling/gear system. Results of two of these studies are listed in Table 2. Neither of these analyses identified forces within the 1270 to 1825 rpm speed range that would excite any of these critical frequencies.

Table 2. Calculated Torsional Critical Speeds for the Motor-Coupling-Gear-Compressor System.

	Frequency, Hz	
MODE	STUDY 1	STUDY 2
1	19.0	19.2
2	33.5	34.1
3	66.3	65.1

Compressor Measurements

Following the second coupling failure, a strain gage type torque transducer was mounted on the motor-to-gear coupling. In October 1991, an eight channel strip chart recorder was installed to continuously record eight parameters, including torque. At the same time, a twenty-one channel tape recorder was installed to record a variety of compressor operating parameters that included torque, pressures, flows, and machine vibration. Eventually, a

computer based data sampling system was used to start the tape recorder when torsional oscillations, speed, or gearbox vibration exceeded preset limits.

Initial measurements showed that the steady-state torque was about 22,000 ft-lbf (264,000 in-lbs). Frequency analysis of the signal showed that a 19.9 Hz oscillating torque with a peak-to-peak amplitude of 500 ft-lb was also present. During November, 1991 several torque excursions were recorded on the strip-chart recorder. Although occasional torsional excursions with higher than normal torsional oscillations were recorded, correlations between the excursions and other parameters were not evident.

On December 4, 1991, the strip-chart recorded an incident in which the torque varied from 0.0 to 30,000 ft-lbf. As shown in Figure 6, this occurred when the motor speed was approximately 1700 rpm. Additional measurements recorded on December 18 and 20 confirmed that high torsional oscillations occurred when the motor speed was 1701 rpm. These torsional oscillations also had a frequency of 19.9 hz. A time of 11.4 minutes is shown in Figure 6 with the peak-to-peak oscillating torque range above 10,000 ft-lbs. This corresponds to 11,680 cycles with a stress range above 3,360 psi. A distribution of the peak-to-peak stress leves for this chart is included in Table 3. A short segment of the trace recorded at a motor speed of 1699 rpm is shown in Figure 7.

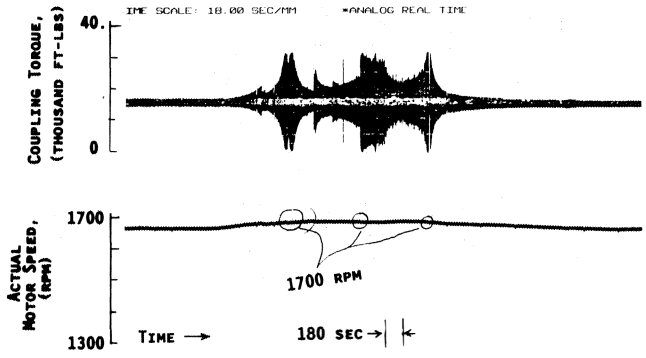

Figure 6. Strip-Chart Recording Showing High Torsional Oscillations Occurring When the Motor Speed Was Approximately 1700 RPM.

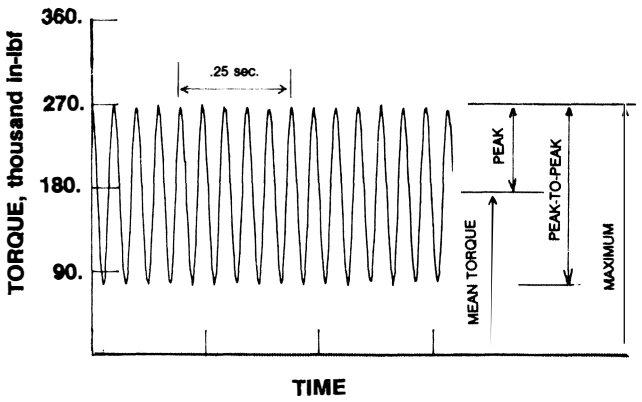

Figure 7. Coupling Torque Recorded at a Motor Speed of 1699 RPM.

Beat Frequency Torsional Excitation

A four pole synchronous motor with variable frequency stator excitation is used to drive the compressor train. With 60 Hz stator excitation, the motor operates at 1800 RPM. When the motor is operating at another speed and the stator frequency is not 60 Hz, beat frequencies are produced at harmonics of the frequency difference (f_n) between line power frequency (60 Hz) and the staror excitation frequency[2]:

$$f_n = 60\text{Hz-Stator Excitation Frequency} \quad (6)$$

where:

$$\text{Stator Excitation Frequency} = 60\text{Hz} * \frac{\text{Rotational Speed}}{1800} \quad (7)$$

These slip frequencies generate torsional pulses at the motor shaft. The six phase, four pole, parallel connection of the compressor motor results in pulses at multiples of six times the frequency difference. As shown in Figure 8 and Equation (8), at 1700 rpm, the $6f_n$ frequency produces 20 Hz pulses that excited the torsional resonance.

$$6f_n = 6*(60\text{Hz}-56.6667\text{Hz}) = 20\text{ Hz} \quad (8)$$

As shown in Figure 9, the peak amplitude of the $6f_n$ pulses are about 0.75 percent of motor output torque at 1700 rpm and the amplitude of the $12f_n$ pulses are about 0.05 percent of motor output torque and is generally harmless.

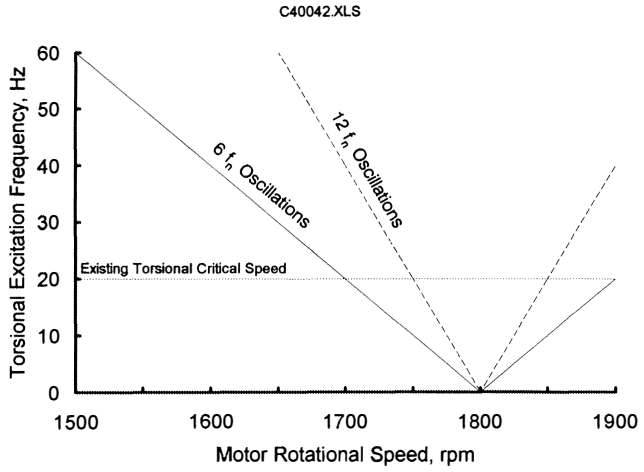

Figure 8. The Relationship Between Motor Rotational Speed and the Subsynchronous Torsional Excitation Frequency. This plot shows that the motor can excite a wide range of torsional critical speeds.

Amplification Factor

On February 5, 1992, when the compressor train experienced high pinion vibration, the tape recorder automatically started and recorded a compressor train shutdown. The step change in torque that occurred when the motor power stopped excited the compressor train torsional resonance and provided a unique opportunity to measure the amplification factor of the torsional resonance. The coupling torsional oscillations recorded during the coastdown are shown in Figure 10.

The decay rate of the torsional oscillations shown in Figure 10 was used to find the damping of the system. Measured peak-to-peak values of the first and fiftieth cycles from Figure 10 were used to find the log decrement and a dynamic amplification factor of 110 for the torsional system, which corresponds to 0.45 percent of

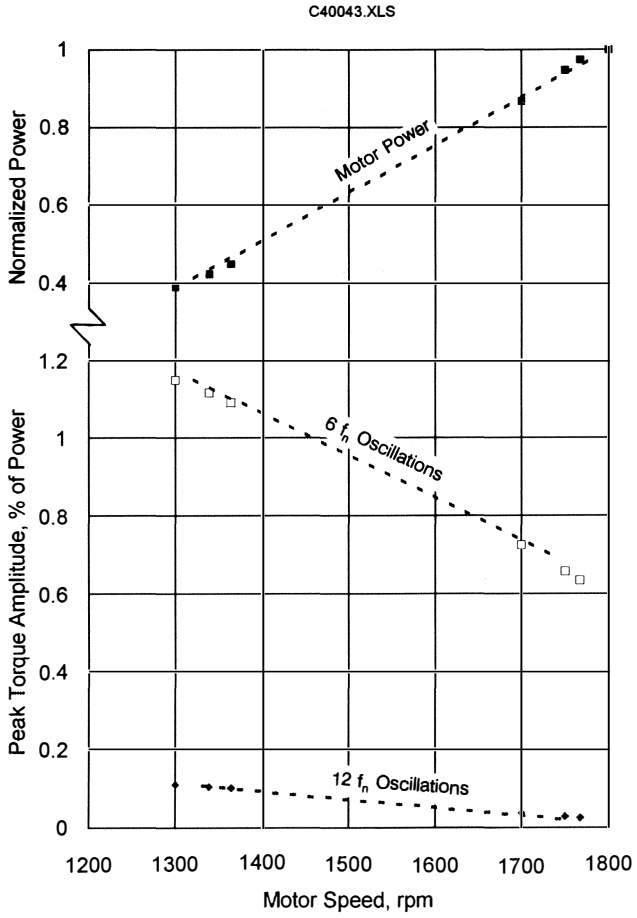

Figure 9. Compressor Train Motor Torque Characteristics Showing Normalized Motor Power (kW) and Peak Torsional Oscillations as a Percent of Motor Power.

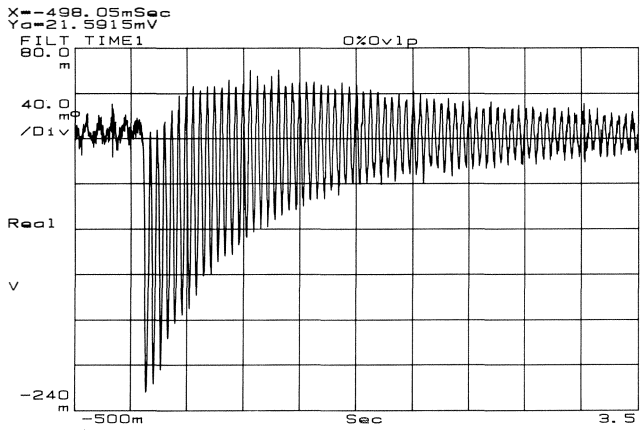

Figure 10. Decay Rate of the Torsional Oscillations Recorded on February 5, 1992.

critical damping. Similar damping values were obtained using the width of the half-power points on several resonance curves that were measured on frequency analysis plots.

The dynamic amplification factor is the ratio of the dynamic coupling torque to dynamic torque pulses produced in the motor. Using the motor peak-to-peak pulse amplitude of 275 in-lb that was predicted by the motor manufacturer as the input, the amplification factor of 110 increases this to 30,250 in-lbs at the coupling, which is close to the values shown in Figure 6.

FINAL VERIFICATION

The final step in the analysis involved showing that a sufficient number of high amplitude torsional cycles had occurred to exceed the fatigue strength of the coupling shown by the curves in Figure 5.

Miner's equation [11] was used to estimate the cumulative damage caused by a given number of cycles at different stress ranges. This equation assumes that for each stress amplitude a linear rate of fatigue damage occurs and failure occurs when the sum of the damage at the various stress levels is 1.0. Thus, if the fatigue life of a component as a stress level of s_1 is N_1 cycles, and that the component experiences N_1' cycles at the stress level s_1 then the cycles have consumed the fraction N_1'/N_1 of the fatigue life. From this, failure occurs when the sum of the proportions of the stress life at each stress range equals 1.0:

$$\frac{N_1'}{N_1} + \frac{N_2'}{N_2} + \frac{N_3'}{N_3} + \ldots = 1 \qquad (9)$$

Although questions exist about the absolute accuracy of Miner's equation, it is adequate for showing that a sufficient number of stress cycles were encountered to cause the failures.

During December 1991and January 1992 six incidents occurred that resulted in stress levels that exceeded the threshold level. The stress amplitude ranges recorded, the number of cycles at each stress range, and the proportion of the coupling fatigue life for each of these events are listed in Table 3. The fraction of the total of the life that occurred during these two months was 0.53 or a half of the life predicted by Miner's equation. (However, it should be noted that this was probably a higher than normal occurrence of incidents. Since then the measurements show fewer incidents per month.)

Table 3. Cumulative Coupling Stress Cycles for December 1991 and January 1992.

	Amplitude (range)			
Date	Torque (ft/lbs)	Stress (psi)	No. Cycles	Fraction of Life
12/04/91	10,000	3,360	18,400	.005
	20,000	6,700	2,100	.005
	25,000	8,400	1,800	.009
	30,000	10,800	1,400	.014
12/15/91	10,000	3,360	54,000	.027
	15,000	5,040	5,000	.007
	25,000	8,400	2,200	.011
12/18/91	25,000	8,400	26,000	.130
	30,000	10,800	17,300	.173
	34,000	11,428	3,000	.043
12/20/91	15,000	5,040	5,000	.007
	34,000	11,428	4,000	.061
01/14/92	25,000	8,400	4,000	.020
01/15/92	20,000	6,700	7,200	.018
			TOTAL	.530

SUMMARY

Starting in the fall of 1991, an organized root cause analysis was conducted on the two coupling failures. This analysis systematically investigated both the failure mechanism and the external forces that acted on the coupling to cause the coupling stresses that resulted in the failures. Verification of the causes consisted of showing that the conditions that were identified as causes of the failures were actually present. The investigation identified three causes that acted together to cause the two coupling failures. These causes are:

• The motor/coupling/bull-gear system has a 19.9 Hz torsional resonance with an amplification factor of 110. This frequency was predicted by torsional studies done before the existing motor-gearbox-compressor system was installed, but the studies did not identify a source that would excite this resonance.

• The motor generates pulses at a subsynchronous beat frequency that excite the 19.9 Hz torsional critical speed. When the motor speed is 1701 rpm, which is within the normal motor operating speed range, this beat frequency excites the 19.9 Hz torsional resonance. Existence of this exciting force was first confirmed by the motor manufacturer in November 1991. Peak-to-peak amplitude of the oscillating torque is approximately 1.5 percent of the design torque of the motor.

• The weld in the coupling provided the weak link in the system. Inspection of the coupling failures showed that the failure cracks started at 0.03 in and 0.06 in inclusions in the welds that connected the coupling diaphragms to the coupling tubes shown in Figure 3. The toe or root of the single V weld that connected the diaphragm to the tube, shown in Figure 3, was at the internal radius formed at the 90 degree junction of these two components. The toe of the weld, where the cracks started, had a high stress concentration factor. Once initiated the crack propagated along the tube and up the diaphragm until the train was shut down due to high motor and gearbox lateral vibration.

To correct the identified causes several corrective actions are being taken:

· The torque transducer, orginally installed to help identify the problem causes, is being connected to a meter in the control room that will monitor oscillation torque.

· Operator intervention is being used to aviod operating the train in the very restricted speed range where the peak oscillating torque exceeds allowable longterm stress limits of the gearbox. This corresponds to a motor speed range of approximately 1696 to 1703 rpm.

· The coupling was redesigned to move the weld away from the high stress concentration region and to increase the coupling's tolorance for torsional vibration.

REFERENCES

1. Mancuso, J. R., Gibbons, C. B., and Munyon, R. E., "The Application of Flexible Couplings for Turbomachinery," *Proceedings of the Eighteenth Turbomachinery Symposium*, The Turbomachinery Laboratory, The Texas A&M University System, College Station, Texas., p. 149 (1989).
2. Grgic, A., Heil, W., and Prenner, H., "Large Converter-Fed Adjustable Speed AC Drives for Turbomachines," *Proceedings of the 21st Turbomachinery Symposium*, The Turbomachinery Laboratory, The Texas A&M University System, College Station, Texas., p. 103 (1992).
3. Hudson, J. H., "Lateral Vibration Created By Torsional Coupling Of A Centrifugal Compressor System Driven By A Current Source Drive For A Variable Speed Induction Motor," *Proceedings of the Twentyfirst Turbomachinery Symposium*, The Turbomachinery Laboratory, The Texas A&M University System, College Station, Texas. p. 103 (1992).
4. Kepner, C. H. and Tregoe, B. B., *The Rational Manager—A Systematic Approach to Problem Solving and Decision Making*, Kepner-Tregoe, Inc., pp. 72-130 (1976).
5. Deutschman, A. D., Michels, W. J., and Wilson, C. E., *Machine Design*, New York, New York: Macmillan Publishing Co., Inc., p. 107 (1975).
6. Shigley, J. E. and Mitchell, L. D., *Mechanical Engineering Design*, New York, New York: McGraw-Hill Book Company, pp. 330-332 (1983).
7. Lipson, C. and Juvinall, R. C., *Handbook of Stress and Strength—Design and Material Applications*, New York, New York: The Macmillan Company, p. 219 (1963).
8. Peterson, R. E., *Stress Concentration Factors*, Wiley-Interscience Publication, p. 106 (1974).
9. Bannantine, J. A. Comer, J. J., and Handrock, J. L., *Fundamentals of Metal Fatigue Analysis*, Englewood Cliffs, New Jersey: Prentice-Hall, pp. 100-114 (1990).
10. Barsom, J. M. and Rolfe, S. T., *Fracture And Fatigue Control In Structures*, Englewood Cliffs, New Jersey: Prentice-Hall, Inc., p. 285 (1987).
11. Spotts, M. F., *Design of Machine Elements*, Englewood Cliffs, New Jersey: Prentice-Hill, Inc. p. 98 (1971).

ACKNOWLEDGEMENTS

The cause analysis of this problem was a mulitdisciplinary effort that required contributions from numerous individuals. In particular Kevin Keyser, Tom Mikus, Herman Storey, and Lee Speicher made significant contributions that helped identify the causes of the coupling failures.